Proposed experiment to assess operation of quantum cellular automaton cells

Massimo Macucci
Dipartimento di Ingegneria dell'Informazione: Elettronica, Informatica, Telecomunicazioni, Università di Pisa
M. Gattobigio
Dipartimento di Ingegneria dell'Informazione: Elettronica, Informatica, Telecomunicazioni, Università di Pisa
Giuseppe Iannaccone
Dipartimento di Ingegneria dell'Informazione: Elettronica, Informatica, Telecomunicazioni, Università di Pisa

M. Macucci, M. Gattobigio, G. Iannaccone, *Proposed experiment to assess operation of quantum cellular automaton cells*, Journal of Applied Physics, **, 17** (45), p.261 (2001).

Proposed experiment to assess operation of quantum cellular automaton cells

M. Macucci,[a] M. Gattobigio, and G. Iannaccone
Dipartimento di Ingegneria dell'Informazione, Università di Pisa, Via Diotisalvi 2, I-56126 Pisa, Italy

(Received 3 January 2001; accepted for publication 12 September 2001)

We propose an experiment for the detection of quantum cellular automaton (QCA) operation in a cell made up of four silicon quantum dots. We show that correlated switching between the two pairs of dots forming the cell can be clearly detected from the locking of the Coulomb blockade current peaks through each pair. We have performed numerical simulations on the basis of capacitance values obtained from experimental results on cells fabricated with silicon-on-insulator technology. This approach is shown to allow detection of QCA switching without the need for additional charge detectors, although fabrication parameters are rather critical. © *2001 American Institute of Physics*. [DOI: 10.1063/1.1416856]

I. INTRODUCTION

During the last decade the concept of logic circuits based on the new paradigm of quantum cellular automata (QCA) has received considerable attention, due to the perspectives of extremely dense integration and of very low power consumption that it appeared to offer. This new computational paradigm was first proposed by Lent *et al.*,[1,2] who realized the possibility of obtaining a strongly bistable behavior by exploiting the properties of electrons confined in nanostructures.

The basic building block of a QCA circuit is represented by a cell made up of four quantum dots arranged at the vertices of a square, and containing two electrons, which can tunnel between dots. The electrons will align along one of the two diagonals, giving rise to two possible polarization states, which can be used to encode the two binary logic values. Polarization propagates between adjacent cells via Coulomb interaction, and this allows transferring logic values along a chain of cells and, more in general, obtaining combinatorial circuits by assembling cells into properly structured two-dimensional arrays.[3] In principle, QCA operation can be obtained without net current flow in the circuit, because the two electrons belonging to each cell may be prevented from tunneling to nearby cells, which leads to extremely low power consumption. In order to achieve such a regime of operation, however, complex technological problems need to be solved, in particular that of loading exactly two electrons in each cell and that of detecting the occupancy of each dot in a noninvasive way.

Actual measurements on QCA prototypes however have been performed with cells in which electrons are loaded via external leads (with the exception of a recent experiment by the Notre Dame group[4]), and therefore a nonzero current flows through the device. Careful adjustment of the voltages applied to the various leads is also needed, in order to compensate for fabrication tolerances, to which QCA devices are extremely sensitive,[5] and to bias the cells exactly on the edge between two different regions of the charging diagram.

The first realization of a QCA cell[6,7] was based on metallic Al islands connected by tunnel barriers ($Al/AlO_x/Al$), and polarization measurements were performed by means of a noninvasive electrometer consisting of a single electron transistor (SET) capacitively coupled to the active islands. Another possible implementation of QCA cells consists of quantum dot cells fabricated on a GaAs/AlGaAs heterostructure. In this case the noninvasive measurement of each dot occupation number has been performed by observing the variation of the resistance of a nearby quantum point contact.[8]

One further attempted implementation of QCA cells is based on silicon-on-insulator (SOI) quantum dots,[9] that are defined by means of electron beam lithography, and are then reduced in size by performing successive oxidation steps. The advantage of such an approach consists mainly of the possibility of fabricating extremely small structures in a reproducible way. The implementation of a QCA cell with metal SETs described in Refs. 6 and 7 is the size of a few micrometers, the prototype cell in GaAs/AlGaAs is about a micron wide, while the prototype cell in SOI technology occupies only a few hundred nanometers and has an active region of just 100×100 nm^2. It would be possible to fabricate charge detectors, in the form of single electron transistors, also within silicon technology, but the complex adjustment that is already needed for a simple cell without a detector would become prohibitive, should the detectors be included, too.

We have therefore devised a measurement scheme that allows demonstration of QCA cell switching, i.e., correlated inverse transfer of electrons between the dots belonging to the two nearby pairs in a cell, without requiring charge detectors, simply with the observation of the variations in the currents flowing through the two dot pairs. In order to obtain the quantitative data needed to turn our concept into the design of a practical experiment, we have developed a specifically tailored Monte Carlo simulator, after some preliminary

[a]Author to whom correspondence should be addressed; electronic mail: massimo@mercurio.iet.unipi.it

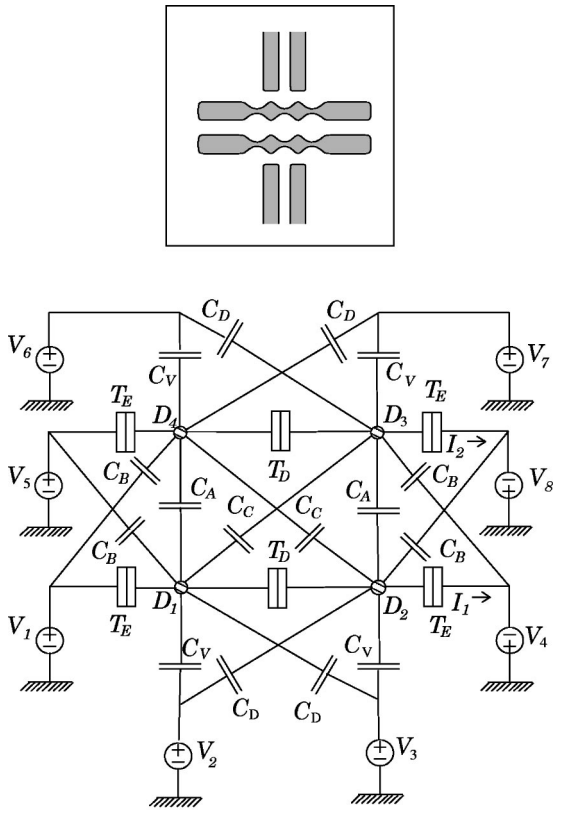

FIG. 1. Equivalent circuit diagram of an SOI QCA cell.

work done with the public domain version of the SIMON SET simulator.[10]

The article is organized as follows: in Sec. II we describe the concept of operation for our proposed experiment, focusing our discussion on a SOI QCA cell. In Sec. III we discuss the operation of our Monte Carlo simulator, while in Sec. IV we show a practical example based on a cell whose capacitance matrix has been obtained from experimental data[11] and from the proposed device layout by means of the FASTCAP code.[12] The effects of lowered coupling capacitances, of temperature, and of asymmetries are discussed, too. Section V is devoted to conclusions.

II. CONCEPT OF OPERATION

Throughout the description of our experiment, we will refer to the structure shown in the inset of Fig. 1, consisting of two pairs of silicon quantum dots with four capacitively coupled adjustment gates. The dots in each pair are defined by means of lithographic constrictions that create tunneling barriers[13] and are connected, via the outer constrictions, to external leads.

This structure can be represented with an equivalent circuit made up of tunneling capacitors and ideal capacitors, as indicated in Fig. 1. The adjustment gates, connected to the voltage sources V_2, V_3, V_6, and V_7, are coupled to the quantum dots, corresponding to nodes D_1, D_2, D_3, and D_4, respectively, through the ideal capacitors C_V. The dots in the same pair are coupled to each other via the tunneling junctions T_D and to external leads via the tunneling junctions T_E. The capacitances between the corresponding dots of the upper and lower pair are represented by the C_A capacitors. The cross capacitances between dots D_1 and D_4, and between dots D_2 and D_3, are indicated with C_C. For the sake of graphic simplification, we have not included in Fig. 1 the capacitances between each adjustment electrode and the dots in the opposite section, although they have been taken into consideration in our calculations, as will be detailed in the following. We indicate the capacitance between a lead and the corresponding dot in the opposite pair (such as the one between V_2 and D_4) as C_K and that between a lead and the diagonally opposite dot (such as the one between V_2 and D_3) as C_J.

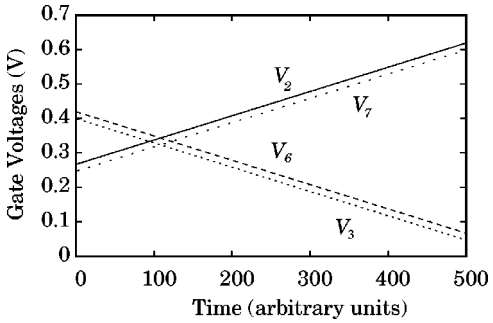

FIG. 2. Time evolution of the voltage ramps applied to the adjustment gates.

Let us first consider the operation of only one pair of dots, for example dots D_1 and D_2 (let us suppose that all the voltage sources connected to the upper dots are kept grounded). By varying the voltage applied to the corresponding adjustment electrodes, it is possible to increase or decrease the number of electrons stored in the quantum dots. If a very small voltage is applied between the left and right lead, a significant current I_1 will flow only if the two dots are brought at the same time at the edge between two stable occupancies, thus lifting the Coulomb blockade. Since we consider the situation of very small voltage values applied between the two outer leads of each double-dot structure, the Coulomb blockade is lifted when the chemical potentials in the two dots line up with those in the leads.

Let us suppose that voltage ramps with opposite slopes (positive for the left dot) are applied to the two adjustment gates V_2 and V_3 (see Fig. 2) and tuned in such a way as to obtain switching from $N-1$ to N electrons in the left dot at the same time as switching from $M+1$ to M electrons in the right dot. This condition is represented in Fig. 3, where the evolution of the left (right) dot occupancy as the gate voltages vary is reported with a dashed (solid) curve. The variation of the applied voltages is assumed to be very slow in comparison with the relevant time scales of the circuit as defined by the tunneling rates and by the RC time constants, therefore the evolution is quasistatic. The results in Fig. 3 have been obtained with the device parameters used to obtain the first set of results of Sec. IV.

The current I_1 through the lower dots will exhibit a peak every time a synchronized variation of the occupancy of the two dots occurs. We can repeat the same measurement on the upper dots, with the voltage sources connected to the lower pair of dots grounded, this time applying a ramp with positive slope to the right gate V_7 and a ramp with negative slope

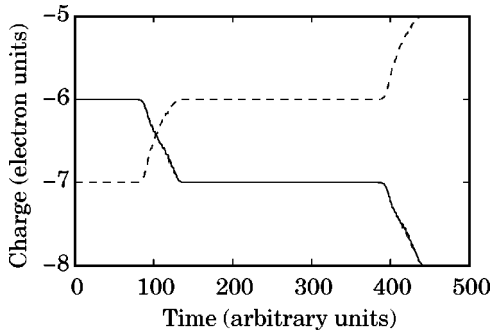

FIG. 3. Time evolution of the number of excess electrons in the lower left (dashed line) and lower right (solid line) dots.

to the left gate V_6, as shown in Fig. 2. We also introduce some shift with respect to the voltages used for the lower dots, so that the current peaks for I_2 will be somewhat displaced with respect to those obtained for I_1.

If we then repeat the experiment with both the upper and the lower section active, electrostatic coupling between the dots will synchronize the transition of an excess electron between the upper dots and the opposite transition between the lower dots, thus leading to a "locking" effect of the current peaks and to the demonstration of cell operation. In other words, while the current peaks occur at different time instants in the upper and lower sections when there is no coupling, the presence of coupling will make them occur at the same time, notwithstanding the shift introduced between the ramp pairs belonging to the two sections. We point out that, in our representation, time is just a conventional parameter, while the actual dependence of the currents is on gate voltages, which are, however, all assumed to vary linearly in time, which justifies usage of time as a single common parameter that can be represented in arbitrary units. In an actual experiment the time evolution of the gate voltages should be slow enough to allow a number of averages in the measurement of currents sufficient to get the accuracy needed for comparison with the theoretical results. Peak displacement and locking is discussed more in detail with the help of simulation results in Sec. IV. Correlated transport between two double dots has also been investigated in Ref. 14, but from the point of view of conductance suppression that occurs if both double dots are biased to conduct at the same time.

III. SIMULATION

For the simulation we follow a semiclassical approach, in the framework of the orthodox Coulomb blockade theory, since quantum effects associated with the confinement energy can be neglected, as a consequence of such energy being much smaller than the electrostatic interaction energy, at the dimensional scale being considered.

Our preliminary calculations were performed with the public domain version of the SIMON program[10] that allows simulating circuits made up of capacitors, tunneling capacitors and voltage sources. Due to some limitations of this version of SIMON in handling relatively large circuits and to the need for a better control of internal simulator parameters, we have developed our own Monte Carlo code for the simulation of single electron circuits, specifically suited to the task of investigating QCA cells. The program is supplied with the capacitance matrix, the position and resistance of tunneling capacitors, the voltages applied to external leads, the gate voltage ramps, and the temperature.

Our code is based on a semistatic Monte Carlo technique: the simulation is divided into a given number of steps and, for each step, we first evaluate the adjustment gate voltages according to the linear evolution rule defined in the input file, then we compute the variation of the free energy ΔE associated with each possible single-electron transition through the tunneling junctions.

Once the free energy variations have been determined, we can compute the corresponding probability rates utilizing the "orthodox" Coulomb blockade theory[15]

$$\Gamma = \frac{1}{e^2 R_T} \frac{\Delta E}{1 - e^{-(\Delta E/k_B)T}}, \tag{1}$$

where R_T is the tunneling resistance, e the electron charge, k_B the Boltzmann constant, and T the temperature.

If we indicate the sum of the tunneling rates Γ_i for each possible transition with Γ_{tot}, constant in time, the probability density function for the random variable representing the time interval Δt between two consecutive transitions is exponential and given by

$$f(\Delta t) = \Gamma_{\text{tot}} e^{-\Gamma_{\text{tot}} \Delta t}. \tag{2}$$

On the basis of Eq. (2), the time interval Δt at each simulation step can be obtained starting from a random number r uniformly distributed in the [0,1] interval, according to[16]

$$\Delta t = -\frac{\ln(r)}{\Gamma_{\text{tot}}}. \tag{3}$$

We then proceed dividing the interval [0,1] into subintervals with amplitude proportional to the different transition rates, and the transition event that has actually taken place is selected by generating another random number r' uniformly distributed in [0,1] and determining the subinterval to which it belongs. Then a new time interval is generated and the procedure is repeated using the new charge configuration, resulting from the previously selected transition, to compute the new transition rates.

This cycle is performed an assigned number of times, sufficient to acquire statistically valid estimators. The charge in each dot is obtained by averaging over all transitions, and the current through each junction is computed as the ratio of the total charge that has traversed the junction to the total elapsed time.

Once estimators for the dot charges and for the junction currents have been obtained, we move on to the next gate voltage configuration, and the same procedure is repeated for all time steps.

IV. RESULTS AND DESIGN

In order to simulate the proposed experiment, we first need to estimate the values of the capacitances and of the tunnel resistances to be included in the circuit model.

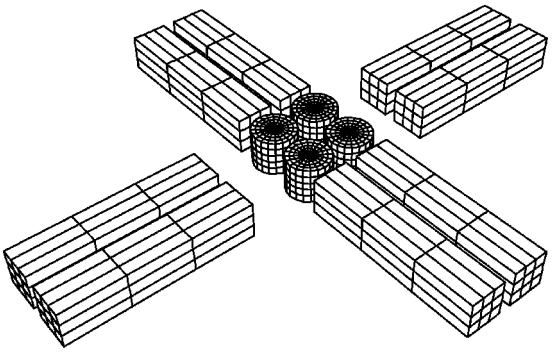

FIG. 4. Schematic representation of the experimental setup used for calculating the capacitance matrix with FASTCAP.

The tunneling junction capacitances cannot be estimated from the device geometry because they are strongly influenced by the potential fluctuations due to the donor atoms.[9] They depend on the detailed behavior of the conduction band edge, which is connected both to the actual lithographic characteristics and to the impurity distribution. For these capacitances we have used experimental values recently obtained by Prins and Kern[11] $T_E=9$ aF and $T=10$ aF. Such values are relatively large, and pose a severe limit to the maximum operating temperature, as we shall see in the following.

The geometrical capacitances, i.e., those between the adjustment gates and the dots, and between the upper and lower dots, have been computed with the FASTCAP program,[12] on the basis of a geometrically idealized representation.

The dots have been modeled as cylinders with a diameter of 60 nm and a thickness of 50 nm, while the leads are represented with parallelepiped stripes $50\times50\times250$ nm^3. The distance between the centers of the dots is 67.5 nm, while that between the dot centers and the edges of the adjustment leads is 105 nm. The separation between the upper and lower dot centers (67.5 nm) is extremely small, but it was chosen in order to get values of C_A close to those of the tunneling capacitances, a necessary condition for proper operation, as will be discussed in the following. A relative permittivity of 4 corresponding to that of silicon oxide has been assumed, considering that the lithographically defined silicon nanostructures are substantially embedded in the oxide.

The FASTCAP model is represented in Fig. 4, with a number of panels smaller, for the sake of graphical clarity, than the actual number used for the discretization of the surfaces (600 panels for the leads and 900 panels for the dots).

The results for the geometrical capacitances from FASTCAP are, with reference to Fig. 1, $C_D=0.92$ aF, $C_V=1.7$ aF, $C_B=1.2$ aF, $C_C=0.95$ aF, and $C_A=9.8$ aF. The previously mentioned cross capacitances C_K and C_J that have not been indicated in Fig. 1 have also been computed and included in the simulation: $C_K=0.25$ aF and $C_J=0.21$ aF.

For all tunneling junctions a resistance of 5 MΩ has been assumed. Due to the relatively large capacitance values, our first calculation has been performed for a temperature of just 0.3 K, in order to prevent thermal smearing of the Coulomb blockade.

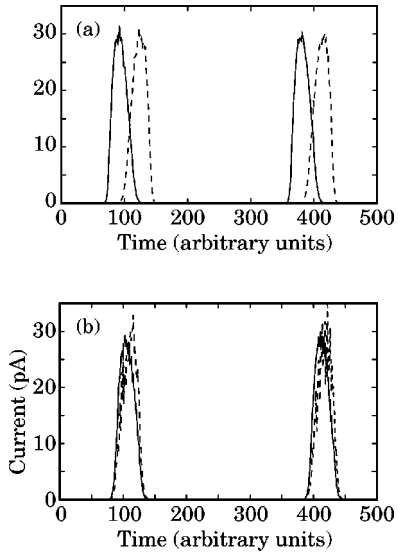

FIG. 5. Currents in the upper (solid line) and in the lower (dashed line) section, for a temperature of 0.3 K, and an interdot distance of 67.5 nm, when each section is operated independently from the other (a) and when the two sections are operated at the same time (b).

Initially $V_5=V_6=V_7=V_8$ are set to zero, thus disabling the upper section of the cell, while voltage ramps with opposite slopes are applied to the control leads of the lower section (V_2 and V_3) as shown in Fig. 2. The relative shift between the ramps is adjusted in such a way as to obtain opposite transitions for the occupancies in the lower two dots at the same time, as discussed in Sec. II. The voltage sources connected to the outer leads of the currently active section, V_1 and V_4, are set to 1 mV. The resulting current I_1, flowing through the lower section, is shown in Fig. 5(a) with a dashed line.

Then the same procedure is repeated operating only the upper section, i.e., setting $V_1=V_2=V_3=V_4=0$, $V_5=V_8=1$ mV, and applying voltage ramps to the upper control leads (V_6 and V_7) with the same slopes as V_3 and V_2, but with a 20 mV shift, which results in current peaks for I_2 [reported with a solid line in Fig. 5(a)] that are displaced with respect to those for I_1.

Finally, the upper and lower sections are operated simultaneously, obtaining the currents I_1 and I_2 reported in Fig. 5(b). The presence of the electrostatic coupling due to the capacitors C_A and C_C leads to a "locking" effect between the peaks in the two currents, i.e., the peaks shift in such a way as to synchronize those in I_1 with those in I_2, as can be seen comparing Figs. 5(a) and 5(b). This is a direct consequence of the correlation between tunneling events of electrons between the upper and the lower dots, a phenomenon exactly equivalent to the operation of a basic QCA cell, with the two "excess" electrons lining up along either diagonal, in response to an external electric field.

In order to distinguish, in the actual experiment, between the locked and the unlocked condition, current measurements need to be performed with sufficient precision: this can be achieved by varying the gate voltages slow enough as to allow the necessary averaging time for each data point.

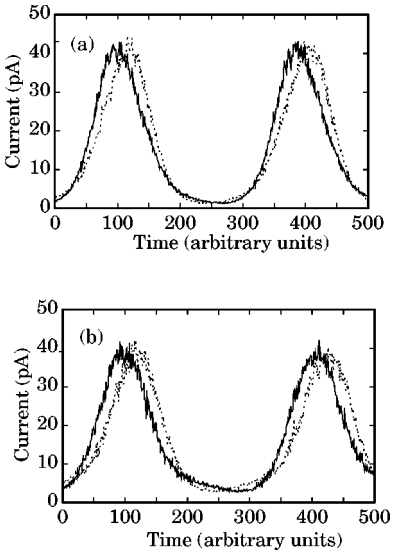

FIG. 6. Currents in the upper (solid line) and in the lower (dotted line) section, for a temperature of 4.2 K, when each section is operated independently from the other (a) and when the two sections are operated at the same time (b).

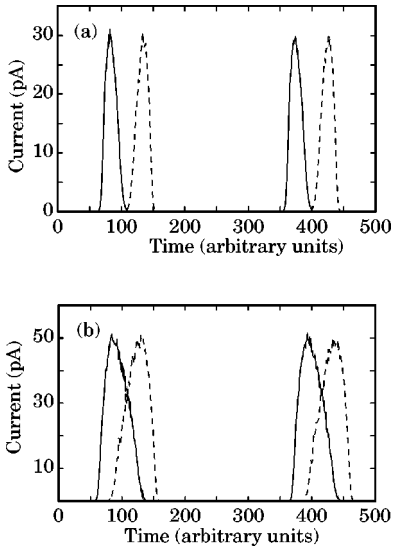

FIG. 7. Currents in the upper (solid line) and in the lower (dashed line) section, for a temperature of 0.3 K and the capacitance between the dots decreased down to 1 aF, when each section is operated independently from the other (a) and when the two sections are operated at the same time (b).

The possibility of achieving peak locking is very dependent on circuit parameters, in particular on the ratios of capacitance values, which makes fabrication of an actual sample somewhat challenging. The capacitances C_A, as already mentioned, provide the needed electrostatic coupling between the upper and the lower section of the cell: they therefore need to be large enough with respect to the other relevant capacitance values, otherwise the locking effect cannot be observed. On the other hand, the capacitances C_C and the stray capacitances that connect each voltage source with the corresponding dot in the opposite section (for example that between V_2 and D_4) act against peak locking, since they provide a contribution to each dot potential that is opposite to that of the C_A capacitances. Little can be done to modify these capacitances, since their values are pretty much the result of the geometrical arrangement that we devise to obtain the desired C_A.

In order to obtain a large enough value for C_A, we have assumed that the upper and lower sections are very close together, with a separation of only 7.5 nm between the edges of facing dots. Even such a close spacing may be insufficient if the temperature is raised up to that of liquid helium, 4.2 K. In Fig. 6 we report the currents obtained in a simulated experiment with the same parameters as those for Fig. 5, except for the temperature, which is now 4.2 K. The situation with both halves of the cell operating at the same time [Fig. 6(b)] differs very little from that with the two halves operating independently [Fig. 6(a)], because of the thermal broadening of the peaks. In this case it is impossible to assess whether locking has actually taken place and therefore to demonstrate cell operation.

On the other hand, if we keep the temperature at 0.3 K, but reduce the values of the C_A capacitances down to 1 aF, by increasing the distance between the centers of the upper and the lower dots, the mutual influence between the two sections becomes so small that, once again, no peak locking can be detected, as shown in Fig. 7: in Fig. 7(a) we report the result for separately operated semicells and in Fig. 7(b) that for simultaneous operation. It is apparent that in this condition coupling through the C_A capacitances produces no significant synchronization between the peaks.

We have also investigated the operation of a cell in which some asymmetry has been purposely introduced. In such a case, peak periodicity is disrupted, but the very same experiment described above can be performed looking at a single current peak in each section and at the locking effect between the peak in I_1 and that in I_2. The asymmetry causing the largest disruption is that on the values of the C_V capacitors, because it alters the action of the voltage ramps on the dot potentials. We have considered an increase to 2.7 aF of the value of the C_V capacitor connecting V_2 to D_1, repeating the procedure for finding the proper shift between the two ramps. Results for the two sections operated independently are reported in Fig. 8(a), while Fig. 8(b) shows peak locking when the two sections are operated simultaneously.

In addition, we have tried introducing several combinations of asymmetries on other capacitances, observing perturbations in the operation of the cell smaller than those due to the altered C_V.

V. CONCLUSIONS

We have devised and simulated an experiment allowing detection of QCA action in four-dot cells made on SOI, without the need for additional charge detectors. Our experiment proposal allows us to detect correlated electron switching between the two halves of a QCA cell by looking at the ensuing synchronization between the Coulomb blockade current peaks. A specifically designed Monte Carlo simulator has been developed for testing our concept, and constraints on the values of the circuit parameters have been determined.

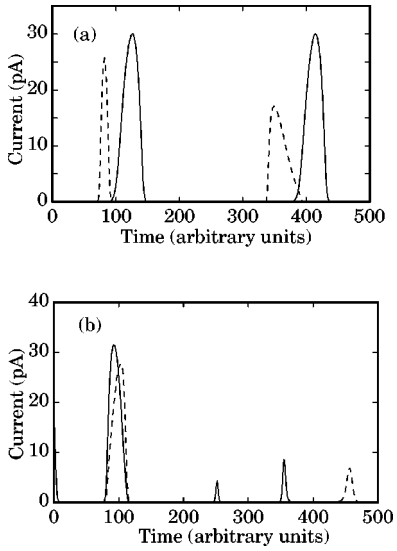

FIG. 8. Currents in the upper (solid line) and in the lower (dashed line) section, for a temperature of 0.3 K and an asymmetry due to a larger value for the capacitor C_V between V_2 and D_1 (2.7 aF), when each section is operated independently from the other (a) and when the two sections are operated at the same time (b).

Fabrication of a structure satisfying the various constraints appears challenging but not impossible with currently available technology.[9] The main difficulty probably consists of obtaining a large enough capacitance between the upper and the lower dots, because this involves a very small spatial separation. Larger distances between the two sections of the cell would be allowed if the capacitances of the tunneling junctions could be reduced, which would also imply the possibility of raising the operating temperature. Simulation results show that the unavoidable asymmetries affecting real cells will not create significant problems for this particular experiment.

Preliminary comparisons between experimental data[9] on SOI nanoelectronic devices and the results of our simulations show good agreement and validate the choice of a model based on the orthodox Coulomb blockade theory. We expect that the proposed experiment will provide verification of the QCA principle on the 100 nm scale, but extension to a complex logic circuit is not likely, both because of the need for adjustment gates, which make difficult the fabrication of neighboring cells with the described layout, and because of the complexity of the unavoidable tuning procedure required for each cell.

Structures and theoretical approaches such as the ones we have presented can however be useful not only for the demonstration of the QCA principle on a nanometric scale, but also to investigate a variety of aspects of correlated transport in single electron systems.

ACKNOWLEDGMENTS

Support from the European Commission, through the ESPRIT Project No. 28667 ANSWERS (Autonomous Nanoelectronic Systems With Extended Replication and Signalling) and No. 23362 QUADRANT (Quantum Devices for Advanced Nano-electronic Technology) is gratefully acknowledged. The authors thank Dr. Freek Prins and Professor Dieter Kern for useful discussion and for providing them with experimental data on the SOI structures.

[1] C.S. Lent, P. D. Tougaw, and W. Porod, Appl. Phys. Lett. **62**, 714 (1993).
[2] C. S. Lent, P. D. Tougaw, W. Porod, and G. H. Bernstein, Nanotechnology **4**, 49 (1993).
[3] P. D. Tougaw and C. S. Lent, J. Appl. Phys. **75**, 1818 (1994).
[4] I. Amlani, A. O. Orlov, R. K. Kummamuru, G. H. Bernstein, C. S. Lent, and G. L. Snider, Appl. Phys. Lett. **77**, 738 (2000).
[5] M. Governale, M. Macucci, G. Iannaccone, C. Ungarelli, and J. Martorell, J. Appl. Phys. **85**, 2962 (1999).
[6] A. O. Orlov, I. Amlani, G. L. Snider, C. S. Lent, and G. H. Bernstein, Appl. Phys. Lett. **72**, 2179 (1998).
[7] I. Amlani, A. O. Orlov, G. Toth, G. H. Bernstein, C. S. Lent, and G. L. Snider, Science **284**, 289 (1999).
[8] C. G. Smith (unpublished).
[9] C. Single, R. Augke, F. E. Prins, D. A. Wharam, and D. P. Kern, Semicond. Sci. Technol. **14**, 1165 (1999).
[10] C. Wasshuber, H. Kosina, and S. Selberherr, IEEE Trans. Comput.-Aided Des. **16**, 937 (1997).
[11] F. E. Prins and D. P. Kern (private communication).
[12] K. Nabors and J. White, IEEE Trans. Comput.-Aided Des. **10**, 1447 (1991).
[13] L. Zhuang, L. Guo, and S. Y. Chou, Appl. Phys. Lett. **72**, 1205 (1998).
[14] G. Tóth, A. O. Orlov, I. Amlani, C. S. Lent, G. H. Bernstein, and G. L. Snider, Phys. Rev. B **60**, 16906 (1999).
[15] D. V. Averin and K. K. Likharev, in *Mesoscopic Phenomena in Solids*, edited by B. L. Altshuler, P. A. Lee, and R. A. Webb (Elsevier, Amsterdam, 1991).
[16] W. H. Press, B. P. Flannery, S. A. Teukolsky, and W. T. Vetterling, *Numerical Recipes* (Cambridge University Press, Cambridge, 1989), p. 200.